Available online at www.sciencedirect.com
SCIENCE DIRECT®
Journal of Nuclear Materials 346 (2005) 48–55
journal of nuclear materials
www.elsevier.com/locate/jnucmat

Enhanced diffusion under alpha self-irradiation in spent nuclear fuel: Theoretical approaches

Cécile Ferry [a,*], Patrick Lovera [a], Christophe Poinssot [a], Philippe Garcia [b]

[a] CEA, Nuclear Energy Division, Department of Physico-Chemistry, CEA-Saclay, B.P. 11, 91 191 Gif-sur-Yvette cedex, France
[b] CEA, Nuclear Energy Division, Department of Nuclear Fuel Studies, CEA-Cadarache, 13108 Saint-Paul Lez Durance cedex, France

Abstract

Various theoretical approaches have been developed in order to estimate the enhanced diffusion coefficient of fission products under alpha self-irradiation in spent nuclear fuel. These simplified models calculate the effects of alpha particles and recoil atoms on mobility of uranium atoms in UO_2. They lead to a diffusion coefficient which is proportional to the volume alpha activity with a proportionality factor of about 10^{-44} (m^5). However, the same models applied for fission lead to a radiation-enhanced diffusion coefficient which is approximately two orders of magnitude lower than values reported in literature for U and Pu. Other models are based on an extrapolation of radiation-enhanced diffusion measured either in reactors or under heavy ion bombardment. These models lead to a proportionality factor between the alpha self-irradiation enhanced diffusion coefficient and the volume alpha activity of 2×10^{-41} (m^5).

PACS: 28.41.K; 66.30; 61.80

1. Introduction

Long-term interim dry storage and underground geological disposal are two of the options studied in France for the management of spent nuclear fuel. Studies are on-going in the framework of the PRECCI program (acronym in French for Research Program on Spent Fuel Long-term evolution) in CEA (Commissariat à l'Energie Atomique) and aims at predicting the long-term behaviour of spent nuclear fuel in the various environmental conditions encountered in dry storage or geological disposal. One of the final objectives is to propose radionuclide source term models for performance assessments of various types of spent nuclear fuel under repository conditions.

The release of radionuclides during geological disposal is classically divided into two terms [1]:

(i) an instantaneous release of radionuclides, often referred to as the instant release fraction (IRF); it corresponds to the fraction of the radionuclide inventory released rapidly as soon as water penetrates into the spent fuel rod;
(ii) a slow long-term release which corresponds to the dissolution of the uranium oxide matrix.

* Corresponding author. Tel.: +33 1 69 08 83 65; fax: +33 1 69 08 52 54.
E-mail address: cecile.ferry@cea.fr (C. Ferry).

0022-3115/$ - see front matter © 2005 Elsevier B.V. All rights reserved.
doi:10.1016/j.jnucmat.2005.04.072

The first term (IRF) is usually considered to be due to the radionuclides located within the regions of the rod presenting no confinement property in the long term (10 000 years). This fraction depends (i) on the location of the radionuclides inside the fuel rod on removal from the reactor, which is governed by the migration behaviour during irradiation in reactor, and (ii) on their mobility during the repository phase before breaching of the confinement. Therefore, to estimate the IRF it is necessary to determine the diffusion coefficients of radionuclides in conditions prevailing in geological disposal.

The mobility of heavy metal atoms (U,Pu), fission gases and volatiles in reactor has been extensively investigated for performance assessment and safety analysis during reactor operations because of its impact on thermo-mechanical behaviour of the fuel rod during irradiation. Extrapolating Arrhenius relationships given in the literature [2,3] shows that thermal diffusion of heavy metals and fissions products can be considered as negligible at the expected temperatures (<400 °C) over the time frame of both long-term dry storage (~100 years) and geological disposal (>10 000 years). However, studies of creep behaviour and swelling under irradiation have shown that creep and swelling rates of the pellet are markedly increased by irradiation under 1200 °C, where these phenomena are controlled by the low diffusion rate of uranium atoms [4]. Furthermore, direct measurements of uranium diffusion in UO_2 in reactor at 900 °C yielded a diffusion coefficient three to four orders of magnitude higher than the thermal diffusion coefficients [5]. These observations lead to the proposal of another mechanism of diffusion, which is not temperature controlled.

Enhanced diffusion of uranium and plutonium in UO_2 and $(U,Pu)O_2$ under irradiation was studied by Matzke [6]. The author showed that the diffusion coefficient was completely athermal below 1000 °C and was proportional to the fission rate. The same behaviour of the diffusion coefficient was observed by Turnbull et al. [7] for fission gases and volatile fission products.

After irradiation in reactor, the alpha activity is very high in the spent nuclear fuel (10^{15} Bq t_{iHM}^{-1}[1] during the first hundred years of cooling in a UO_2 fuel irradiated to 47.5 GWd t_{iHM}^{-1}). The effects of alpha decay in UO_2 are similar to the effects of fission. Therefore a mechanism of diffusion enhanced by alpha self-irradiation is expected to occur in the spent nuclear fuel out of reactor. This mechanism should be lower by some orders of magnitude than the one measured under fission in reactor. Thus direct measurements of the diffusion enhanced by alpha self-irradiation seem to be not possible within the time frame of laboratory experiments. Various theoretical approaches have been developed in order to propose rough estimates of the alpha self-irradiation enhanced diffusion coefficient. They are presented in this paper. The models are based on the effects of the recoil atom and of the alpha particle in the UO_2 lattice in comparison with the effects of fission fragments and also on the radiation-enhanced diffusion coefficients reported in literature.

Before extrapolating data measured in reactor to out-of-reactor conditions, it seems necessary to identify and quantify the mechanisms which cause the enhanced mobility of atoms observed under fission. Thus, the first part of the paper reviews the experimental data and mechanisms proposed in the literature to explain the enhanced mobility of atoms observed in reactor. The effects of alpha decays in UO_2 matrix are then described and their potential influence on atomic mobility is discussed. The diffusion coefficient corresponding to each particular mechanism is also proposed.

2. Review on enhanced diffusion under fission

2.1. Experimental data

Matzke described in [6] the complete results of the RADIF (*RAD*iation-enhanced *DIF*fusion) experiments performed in the 1980s by the Institute for Transuranium Elements in order to determine the enhanced diffusion coefficients of U and Pu atoms under irradiation. These experiments consisted of measuring diffusion coefficients of isotopic tracers of U and Pu in UO_2 and $(U,Pu)O_2$ during fission in a nuclear reactor. The influence of fission rates (between 7×10^{17} and 6.4×10^{19} fission m^{-3} s^{-1}) and temperature (between 130 and 1400 °C) was studied. The diffusion coefficient was found to be temperature independent below 1000 °C within the limit of measurement precision (see Fig. 3 in [6]).

The relationship between the radiation-enhanced diffusion coefficient of U and Pu in UO_2, D^* (m^2 s^{-1}) and the fission rate, F (fissions m^{-3} s^{-1}) derived from these observations was [6]:

$$D^* = AF \quad \text{with } A = 1.2\times10^{-39}\ \text{m}^5. \tag{1}$$

The radiation-enhanced diffusion coefficients in other nuclear ceramics ((U,Pu)C and (U,Pu)N) were also measured. The results showed that radiation-enhanced diffusion decreases in the order $(U,Pu)O_2 > (U,Pu)C > (U,Pu)N$ and is lower in (U,Pu)C than in $(U,Pu)O_2$ by approximately one order of magnitude [8].

Enhanced diffusion under irradiation was also studied for rare gases (Xe, Kr) and volatiles (I, Br). Experimental data and conditions reported in the literature for these elements are summarized in Table 1. In conclusion, experimental data have evidenced enhanced mobility of atoms due to fission. This mechanism is represented by a diffusion coefficient which is proportional to the fission

[1] t_{iHM} = ton of initial heavy metal.

Table 1
Summary of experimental data on radiation-enhanced diffusion coefficients of rare gases and volatiles in UO_2 reported in literature

Authors	Elements	D^*/F, m^5	Type of determination
Turnbull et al. [7]	Xe, I	2×10^{-40}	Fission gas released during fission
Matzke et al. [9]	Kr	2×10^{-40}	Gas released under heavy ions bombardment
Hocking et al. [10]	I	$0.5–2\times10^{-39}$	Diffusion profile after heavy ions bombardment
Brémier and Walker [11]	Xe	$2\times10^{-43}–2\times10^{-41}$	Steady state xenon concentration in rim grains after restructuring

rate. A large range of values, extending over three orders of magnitude for rare gases (see Table 1), were proposed in the literature. These observed discrepancies may be explained either by an increase of diffusion due to initial implantation defects in some experiments [10] or by a decrease of diffusion due to trapping of gas atoms in bubbles in other experiments [7,11]. Damage in UO_2 induced by the fission fragments, which could explain the excess mobility of atoms, is discussed below.

2.2. Mechanisms of enhanced diffusion under fission

The fission fragments are decelerated in the lattice over a mean distance of about 8 μm in oxide fuel. Over most of its path length (first 5–6 μm), each fission fragment transfers its energy (96%) by ionization and electronic excitation. In the final micrometers, it releases the remaining energy (4%) by nuclear collisions which create atomic displacement cascades in the lattice [8].

The instantaneous effects of fission fragments are summarized in Table 2. They occur over a very short time interval ($\sim10^{-11}$ s). The thermal spike associated with each fission fragment leads to a significant temperature rise along its path in a fuel volume of about 10^{-16}–10^{-15} cm^3 with the simultaneous formation in this volume of a thermo-elastic pressure field of 5×10^2 to 10^3 MPa due to thermal expansion [13]. These thermal and mechanical effects considerably amplify the recombination and mobility of the Frenkel pairs initially created by fission. According to [14], 80% of uranium Frenkel pairs created during fission disappear by recombination during the thermal spike.

Mechanisms that could be responsible for enhanced diffusion observed under irradiation have been reviewed in [6,8]. Fast neutrons and conventional displacements induced by atomic collisions were calculated to lead to D^* values which are lower by a factor of more than two orders of magnitude than the experimental results given in Eq. (1). Furthermore, no enhanced mobility induced by recovery of defects due to thermal annealing was observed after fission in the RADIF experiments. The thermal rod model initially proposed to explain irradiation-enhanced creep of UO_2 was also reported in [6] as an explanation for the observed D^* values. By considering that a molten volume V (10^{-15} cm^3) caused by the thermal spike exists along the fission spike in UO_2 during a time τ (2×10^{-11} s), the diffusion coefficient D^* is given by:

$$D^* = D_{\text{melt}}\tau VF, \tag{2}$$

where D_{melt} is the diffusion coefficient typical of the melt (i.e. $D_{\text{melt}} \approx 10^{-8}$ m^2 s^{-1}).

Hence, the thermal rod model yields a proportionality factor of 2×10^{-40} m^5 between D^* and F. This value is approximately one order of magnitude lower than the measured value for U and Pu (1.2×10^{-39} m^5) although a high value for the volume of the molten zone was taken into account in the calculation [13]. Matzke [6] concluded then that a more effective mixing than in the thermal rod approach takes place and invoked the large pressure gradient existing along the fission track causing a large separation of Frenkel defects to explain the observed values of enhanced diffusion. These processes should be more important in UO_2 because of its low thermal and electrical conductivity and should be absent in materials like UC. This interpretation is consistent with the difference between the D^* values measured in UC and UO_2 [8].

Table 2
Effects of fission fragments in the UO_2 matrix [8,12]

Type	Energy, keV	Path, μm	Energy fraction lost through elastic collisions, %	Energy fraction lost through electronic excitation, %	Total number of atoms displaced
Light fragment	~95000	9	3	97	~40000 (~10300 U + 27700 O)
Heavy fragment	~70000	7	6	94	~60000 (~16500 U + 45000 O)

3. Enhanced diffusion under alpha self-irradiation

In spent nuclear fuels, the alpha activity is still very high over thousands years after removal from the reactor (see Fig. 1). An enhanced diffusion similar to the one observed under fission but lower by some orders of magnitude is then expected to occur in spent nuclear fuel. The following paragraphs describe the theoretical models that were developed in order to quantify the effects of alpha decays in UO_2. Their influence on atoms mobility is then discussed. The diffusion coefficient corresponding to each depicted mechanism is roughly assessed. In the proposed models, spent fuel is considered to be similar to UO_2, i.e. properties of UO_2 are used to assess the diffusion coefficients of U and O in UO_2 in order to simulate the mobility of fission products in spent fuel. The effects of fission products, particularly of fission gas bubbles, irradiation defects and heterogeneity of the spent fuel pellets are thus not taken into account in these simplified models.

3.1. Effects of the alpha decay in UO_2

Damage due to the alpha particle and recoil atom emitted by alpha decays of actinides in UO_2 are summarized in Table 3 in comparison with the characteristics of the fission fragment damage in UO_2. Extrapolation from in-reactor data given by Eq. (1) was already proposed by the authors in order to assess the diffusion coefficient enhanced by alpha self-irradiation [16]. In this approach, the diffusion coefficient was assumed to be proportional to the total number of displaced atoms by each event (fission or alpha decay). It led to a diffusion coefficient enhanced by alpha self-irradiation, D^*_α ($m^2\,s^{-1}$) which is proportional to the volume alpha activity A_α (Bq m^{-3}) as [16]:

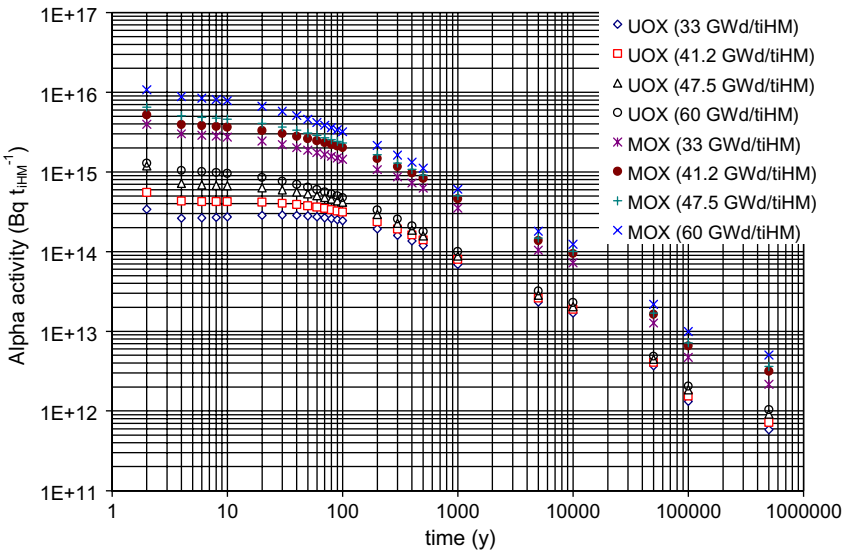

Fig. 1. Specific alpha activities of UO_2 (UOX) and MOX fuels versus time and burnup calculated with the code CESAR4 [15].

Table 3
Effects of fission fragments, alpha particle and recoil atom in UO_2 [12]

Parameter	Fission fragment	α particle	Recoil atom
Stopping range	7–9 μm	15 μm	20 nm
Energy	70–95 MeV	5 MeV	~100 keV
Fraction of energy lost by elastic (nuclear)/ inelastic (electronic) collisions	0.04/0.96	0.01/0.99	0.9/0.1
Number of displaced atoms	~4 to 6×10^4[a]	200	~1500[b]

[a] Effective total number of Frenkel pairs (i.e. after recombination) produced by fission $\sim5\times10^3$ [8].
[b] Dynamic molecular simulation of cascades created by a U incident atom of 70 keV yields 290 effective Frenkel pairs of oxygen and 110 effective Frenkel pairs of uranium.

$$D_\alpha^* \approx 2 \times 10^{-41} A_\alpha. \quad (3)$$

This approach is based on a major assumption with a relatively poor physical justification. Therefore, theoretical approaches based more precisely on the potential effects of the recoil nuclei and alpha particles on the mobility of atoms in the UO_2 matrix are proposed here to estimate the diffusion coefficients enhanced by alpha self-irradiation.

3.2. Enhanced mobility induced by elastic collisions

The effects of the elastic collisions due to the recoil nucleus on the mobility of atoms in UO_2 are discussed in this section.

3.2.1. Atomic displacements due to ballistic collisions

The first cause of enhanced mobility is the cascade of displacements created by the recoil atoms: the total number of atoms (uranium and oxygen) displaced per recoil atom ranges from 1100 to 2200 [17] (about 300 U atoms + 850 O atoms displaced by an alpha decay event). Following a random motion, the diffusion coefficient due to ballistic collisions, D_α^{bal}, is given by:

$$D_\alpha^{\text{bal}} = \frac{\delta^2}{2\theta_c}, \quad (4)$$

where δ^2 is the mean square path distance per displacement and θ_c, the characteristic time to achieve one displacement per atom on average. θ_c is related to the total number of U displaced atoms by cascades n_d and to the volume alpha activity by:

$$\theta_c = \frac{\rho \cdot N_{\text{av}}}{M \cdot n_d A_\alpha}, \quad (5)$$

where M is the molar mass of UO_2 (0.270 kg mol^{-1}), ρ its volume mass ($\sim 10^4$ kg m^{-3}) and N_{av}, the Avogadro's number (6.02×10^{23}).

Then a rough estimate of the diffusion coefficient of uranium induced by cascades is given by:

$$D_\alpha^{\text{bal}} = \frac{M}{2\rho \cdot N_{\text{av}}} \delta^2 n_d A_\alpha. \quad (6)$$

Assuming a mean square path length per displacement of 0.30 nm^2 – this value is based on the results of molecular dynamic simulations – Eq. (6) leads to a proportionality coefficient between D_α^{bal} and a volume alpha activity of about 2×10^{-45} m^5 for U atoms.

In reactor, fission fragments lose a small part of their energy by ballistic collisions (see Table 1). The ballistic effects of fissions on U atom mobility can also be assessed by using Eq. (6) with the number of U atoms displaced per fission ($n_d \approx 27000$), the volume fission rate F instead of A_α, and by assuming a mean square path length of 1 nm^2 per displacement. It yields a proportionality coefficient A close to 6×10^{-43} m^5. This value is three to four orders of magnitude lower than the experimental value given in Eq. (1). In agreement with the conclusion given in [6], cascades alone cannot explain the diffusion process observed in reactor. Therefore, other mechanisms of diffusion seem to contribute to the excess mobility of atoms in reactor. It should be also the case for the diffusion process under alpha self-irradiation.

3.2.2. Diffusion accelerated by migration of point defects

In crystalline solids, the atomic mobility at thermal equilibrium is mainly due to defects. Two types of defects can coexist: interstitial defects (one atom inserted in an interstitial position in the crystal) and vacancy defects (one atom absent from its site). The thermal vibrations insure an equilibrium between both types of defects. Irradiation by energetic particles create such defects by moving some atoms from their initial location. However, the created defects are out of equilibrium and their number results from the equilibrium between creation by the flux of irradiating particles and their elimination in wells.

Due to recombination, the number of isolated defects created by the recoil atom is lower than the total number of displaced atoms. The numbers of oxygen and uranium Frenkel pairs created in UO_2 by a uranium incident atom with an energy ranging between 1 keV and 20 keV were calculated by molecular dynamic simulations. Extrapolation of these results to an incident energy of 70 keV yields 290 Frenkel pairs of oxygen and 110 Frenkel pairs of uranium created per recoil atom. The enhanced mobility of atoms due to the thermal annealing of these defects was determined by a very simple model of point-defect migration: the steady-state number of interstitials and vacancies of uranium and oxygen is calculated by taking into account the creation rate given above, a recombination term of Frenkel pairs, and an elimination term of defects at the sinks (grain boundaries, dislocations ...). Table 4 summarizes the enhanced diffusion coefficient of O and U atoms due to the mobility of defects created in excess by alpha decays. The migration of defects is thermally activated, thus the diffusion coefficients given here depend on temperature.

Below 600 K, the mobility of uranium vacancies is very low (10^{-37} m^2 s^{-1}). Thus the enhanced mobility of the fission products which migrate via uranium vacancies or Schottky trio (one uranium + two oxygen vacancies) induced by this process should be negligible. Furthermore, this mechanism of diffusion is temperature dependent, in contrast to the radiation-enhanced diffusion coefficients observed in reactor (see Section 2.1). Thus, it cannot explain the enhanced mobility observed under fission at very low temperature.

Table 4
Increase of the oxygen (D_α^O) and uranium (D_α^U) diffusion coefficients due to the defects created by cascades of displacements versus volume alpha activity and temperature

Volume alpha activity, Bq m^{-3}	10^{16}	10^{15}	10^{14}	10^{13}
D_α^O at 300 K (m^2 s^{-1})	2×10^{-27}	7×10^{-28}	2×10^{-28}	7×10^{-29}
D_α^O at 400 K (m^2 s^{-1})	3×10^{-25}	8×10^{-26}	2×10^{-26}	4×10^{-27}
D_α^O at 600 K (m^2 s^{-1})	5×10^{-24}	5×10^{-25}	5×10^{-26}	5×10^{-27}
D_α^U at 600 K (m^2 s^{-1})	3×10^{-29}	9×10^{-30}	3×10^{-30}	9×10^{-31}

3.3. Enhanced mobility induced by electronic excitation

The effects of inelastic collisions on the mobility of atoms are discussed in this section.

3.3.1. Extrapolation from accelerator data

As with fission fragments, the alpha particle loses most of its energy by inelastic collisions. An interpretation of enhanced diffusion induced by electronic excitation is proposed here by considering that the diffusion coefficient D^* (m^2 s^{-1}) observed in reactor is proportional to the material volume damaged by the two fission fragments per unit material volume:

$$D^* = k_{\mathrm{d}E/\mathrm{d}x} 2\mu F, \tag{7}$$

where μ is the fragment path length in the UO_2 (m) and F, the fission rate (fissions m^{-3} s^{-1}). The $k_{\mathrm{d}E/\mathrm{d}x}$ value for iodine assuming an incident ion stopping power of 20 keV nm^{-1} was estimated on the basis of work performed under irradiation by Hocking et al. [10] and ranges between 4×10^{-35} and 1.4×10^{-34} m^4.

Assuming the proportionality factor $k_{\mathrm{d}E/\mathrm{d}x}$ is linearly dependent on the electronic interaction arising from the incident particles, its value ranges between 6×10^{-37} and 2.1×10^{-36} m^4 for 5 MeV alpha particles with an electronic stopping power of 0.3 keV nm^{-1}. By analogy with the reactor model, the alpha self-irradiation enhanced diffusion coefficient associated with electronic excitation in a material with an alpha volume activity A_α is thus:

$$D_\alpha^E = k_{0.3\ \mathrm{keV/nm}} \mu_\alpha A_\alpha. \tag{8}$$

Allowing for the path length of the alpha particle in UO_2 ($\mu_\alpha \approx 15$ μm), the contribution of electronic excitation to diffusion was inferred for iodine:

$$D_\alpha^E \approx 2\times10^{-41} A_\alpha. \tag{9}$$

This value is the same as the value based on the extrapolation from in-reactor data for uranium (see Section 3.1).

3.3.2. The thermal rod approach

If we assume that electronic excitation due to the alpha particle induces a thermal spike as with fission, the enhanced diffusion can also be evaluated using the thermal rod approach (see Section 2.2). The diffusion coefficient, $D_\alpha^{\mathrm{throd}}$ (m^2 s^{-1}) is then given by:

$$D_\alpha^{\mathrm{throd}} = D_{\mathrm{melt}} \tau V A_\alpha, \tag{10}$$

where D_{melt} is the diffusion coefficient in the melt (see Section 2.2), V is the volume of the molten zone (m^3) and τ its life-time (s).

An analytical model based on a balance of energy (macroscopic approach) has been developed in order to calculate the characteristics of the molten zone induced by the alpha particle and by the recoil atom.

Assuming that the inelastic loss of energy, $E(J)$, creates a molten zone at the melting temperature of UO_2, T_m, the characteristics of the molten zone are given by the energy balance:

$$E = n\int_{T_0}^{T_m} C_p \,\mathrm{d}T + n\Delta H_m \tag{11}$$

with n the number of UO_2 moles in the molten zone; T_0, the initial temperature of the bulk; C_p, the heat capacity of UO_2 (J mol^{-1} K^{-1}) and ΔH_m, the enthalpy of melting (J mol^{-1}). By neglecting the temperature dependence of parameters, we obtain:

$$n = \frac{E}{C_p(T_m - T_0) + \Delta H_m} \tag{12}$$

and the volume of the molten zone is given by:

$$V = \frac{M}{\rho}\frac{E}{C_p(T_m - T_0) + \Delta H_m} \tag{13}$$

with M the molar mass of UO_2 (kg mol^{-1}) and ρ its volume mass (kg m^{-3}).

Eq. (13) neglects the loss of heat in the liquid phase and should lead to an overestimate of V. Its application to fission leads to a volume of the molten zone due to the fission spike of 10^{-15} cm^3, which is in good agreement with the value reported in [13] (see Section 2.2).

The life-time of the molten zone, τ, is then calculated by assuming that the molten zone is a cylinder (*thermal rod*) along the stopping range μ (m) of the damaging particle. The heat of the cylinder dissipates by thermal conduction in the bulk (infinite medium) which is at the constant temperature T_0. The profile of temperature in the medium is then given by [18]:

$$T(r,t) - T_0 = (T_m - T_0)\,\mathrm{erfc}\left(\frac{r}{2\sqrt{at}}\right) \quad \text{with } a = \frac{\lambda\cdot M}{\rho\cdot C_p}, \tag{14}$$

where r is the distance from the cylinder and λ, the thermal conductivity of UO_2 ($W\,m^{-1}\,K^{-1}$). From Fourier's law, the thermal flux at the surface of the cylinder is given by:

$$\varphi = -\lambda \left.\frac{\partial T}{\partial r}\right|_{r=0} = +\lambda \frac{2}{\sqrt{\pi}} \frac{(T_m - T_0)}{2\sqrt{at}} = \frac{\lambda (T_m - T_0)}{\sqrt{\pi a t}}. \quad (15)$$

The life-time of the thermal rod, τ, is then considered as the time during which the latent heat of solidification is transferred to the bulk: it means that the temperature of the molten zone is constant at T_m during the time τ:

$$n\Delta H_m = \int_0^{\tau} \varphi(t) S \,dt = \frac{2\lambda S (T_m - T_0)}{\sqrt{\pi a}} \sqrt{\tau}, \quad (16)$$

where S is the external surface of the cylinder. Then,

$$\tau = \frac{M}{\rho} \frac{(n\Delta H_m)^2}{16\lambda \cdot C_p \cdot \mu \cdot V (T_m - T_0)^2}. \quad (17)$$

Replacing τ and V in Eq. (10) yields:

$$\frac{D_\alpha^{throd}}{A_\alpha} = \frac{M}{\rho} \frac{D_{melt} \cdot n^2 \cdot \Delta H_m^2}{16\lambda \cdot C_p \cdot \mu \cdot (T_m - T_0)^2}. \quad (18)$$

From Eqs. (12) and (18), it appears that the diffusion coefficient calculated by the thermal rod approach is proportional to E^2/μ. Taking into account the electronic loss of energy of the recoil atom and of the alpha particle and their respective stopping ranges in the lattice, the enhanced diffusion induced by electronic excitation is essentially due to the alpha particle. Combining Eqs. (12) and (18) with the values of the parameters reported in Table 5 leads to a proportionality factor between the enhanced diffusion coefficient and the volume alpha activity of $7 \times 10^{-45}\ m^5$, which is of the same order as the diffusion enhanced by ballistic collisions.

Table 5
Values of the parameters used in Eqs. (12) and (18) for alpha decay out-of-reactor and of fission in reactor [19]

Parameter	Value for alpha decay out of reactor	Value for fission in reactor
C_p	123[a] J mol^{-1} K^{-1}	123 J mol^{-1} K^{-1}
λ	3.959 W m^{-1} K^{-1}	3.959 W m^{-1} K^{-1}
ΔH_m	7×10^4 J mol^{-1}	7×10^4 J mol^{-1}
M	0.270 kg mol^{-1}	0.270 kg mol^{-1}
ρ	9560 kg m^3	9560 kg m^3
D_{melt}	10^{-8} m^2 s^{-1}	10^{-8} m^2 s^{-1}
T_m	3120 K	3120 K
T_0	500 K	1000 K
E	8×10^{-13} J for the α particle 1.3×10^{-15} J for the recoil atom	1.4×10^{-11} J Per fission fragment
μ	1.5×10^{-5} m for the α particle 2×10^{-8} m for the recoil atom	9×10^{-6} m

[a] Corresponds to the mean value of C_p between 1000 K and 3120 K.

If this very simplified approach is applied to the characteristics of fissions in reactor that are also given in Table 5, it yields a value of $2 \times 10^{-41}\ m^5$ for A which is in agreement with the value reported in [6] for the thermal rod approach.

4. Synthesis and discussion

The values of the alpha self-irradiation enhanced diffusion coefficients of uranium given by the various

Table 6
Enhanced diffusion coefficients under alpha self-irradiation given by the different theoretical approaches (A_α is the volume alpha activity in Bq m^{-3})

Model	Diffusion coefficient (m^2 s^{-1})	Comments
Extrapolation from in reactor data for uranium	$D_\alpha^* \approx 2 \times 10^{-41} A_\alpha$	D_α^* is proportional to the total number of atoms displaced per alpha decay; extrapolation from fission fragments effects is based on the A value given in [6]
Extrapolation from irradiators data for iodine	$D_\alpha^E \approx 2 \times 10^{-41} A_\alpha$	D_α^E is proportional to the volume damaged by the alpha particle; extrapolation is based on the A value given in [10]
Effect of ballistic collisions for uranium	$D_\alpha^{bal} \approx 2 \times 10^{-45} A_\alpha$	Random motion due to cascades of displacements
Migration of defects		
At 600 K for O	$D_\alpha^O \approx 5 \times 10^{-40} A_\alpha$	Diffusion accelerated by the thermal migration of punctual defects created by cascades
At 400 K for O	$D_\alpha^O \approx 3.5 \times 10^{-35} A_\alpha^{0.62}$	
At 600 K for U	$D_\alpha^U \approx 3 \times 10^{-37} A_\alpha^{0.5}$	
Electronic effect	$D_\alpha^{throd} \approx 7 \times 10^{-45} A_\alpha$	Thermal rod approach

theoretical approaches described above are summarized in Table 6 with the main assumptions of the models.

The physical models based on the enhanced mobility of atoms induced by the alpha particle due to electronic excitation and by the recoil atom due to cascades of displacements yields an enhanced diffusion coefficient for U atoms under alpha self-irradiation, D_α^{tot}:

$$D_\alpha^{tot} = D_\alpha^{throd} + D_\alpha^{bal} \approx 9 \times 10^{-45} A_\alpha. \quad (19)$$

Eq. (19) yields a diffusion coefficient which is fairly constant over the first hundred years (see Fig. 1) and ranges between 2×10^{-29} and $4 \times 10^{-28}\ m^2\ s^{-1}$ depending on the type of fuel (UO_2 or MOX) and the burnup (from 33 to 60 GWd t_{iHM}^{-1}). It then decreases with time as the alpha activity in the spent fuel decreases. However, these models applied for fission do not reproduce the high value of radiation-enhanced diffusion coefficient given in Eq. (1).

The two other models correspond to an extrapolation from in reactor and heavy ion bombardment experimental data reported in [6,10]. Both are based on the highest values reported in the literature for radiation-enhanced diffusion (see Table 1) and should give an upper estimate of D_α which is three orders of magnitude higher than the value given by Eq. (19). It leads to a cumulative fraction released from spherical grains of 8 μm calculated with the Booth's model of about 5% after 10000 years of disposal [20]. It indicates a limited effect of this mechanism on the release of radionuclides from the spent fuel grains in repository conditions, although the value used for the calculation should represent an upper estimate of D_α^*.

5. Conclusion

Rough estimates of the diffusion coefficient enhanced by alpha self-irradiation were proposed. Some were based on an assessment of the electronic effect due to the alpha particle and of the ballistic effects due to the recoil atom on the mobility of U and O atoms in UO_2. These models yield values smaller than $4 \times 10^{-28}\ m^2\ s^{-1}$ for U atoms during the first hundred years of cooling but are not able to reproduce the enhanced mobility observed under fission. Thus, other approaches proposed were based on extrapolation from the highest radiation-enhanced diffusion coefficients reported in the literature. The mean value of the diffusion coefficient deduced from these extrapolations is $10^{-25}\ m^2\ s^{-1}$ during the first hundred years of cooling in a UOX fuel with a burnup of 60 GWd t_{iHM}^{-1}.

Hence, many uncertainties exist concerning the alpha self-irradiation enhanced diffusion coefficient. The on-going experiments should allow to depict the mechanisms of enhanced mobility of He and I atoms under alpha self-irradiation: The 5 MeV alpha particle fluence that would be necessary to measure an atomic displacement within the detection limits of the analysis methods available (NRA or SIMS) is too high; the electronic effect will therefore be studied mainly through irradiation by heavy ions (Xe, Kr, I, Br) – with different higher energy and stopping powers and at various fluences.

Acknowledgments

The authors thank Laurent Van Brutzel for the molecular dynamics simulation and Jean Paul Crocombette for the point-defects model. Many thanks also to L.H. Johnson for his advice. This work was performed in the frame of the PRECCI project of CEA supported by EDF.

References

[1] L. Johnson, N.C. Garisto, S. Stroes-Gascoyne, Proc. Waste Manage 1985 (1985) 479.
[2] Hj. Matzke, J. Chem. Soc. 86 (8) (1990) 1243.
[3] P. Lovera, C. Ferry, C. Poinssot, L. Johnson, CEA Report, CEA-R-6039, 2003.
[4] D. Brucklacher, W. Dienst, J. Nucl. Mater. 42 (1972) 285.
[5] A. Hoh, Hj. Matzke, J. Nucl. Mater. 48 (1973) 157.
[6] Hj. Matzke, Rad. Eff. 75 (1983) 317.
[7] A. Turnbull, C.A. Friskey, J.R. Findlay, F.A. Johnson, A.J. Walter, J. Nucl. Mater. 107 (1982) 168.
[8] Hj. Matzke, Rad. Eff. 64 (1982) 3.
[9] Hj. Matzke, P.G. Lucuta, T. Wiss, Nucl. Instrum. and Meth. B 166–167 (2000) 920.
[10] W.H. Hocking, R.A. Verrall, I.J. Muir, J. Nucl. Mater. 294 (2001) 45.
[11] S. Brémier, C.T. Walker, Rad. Eff. Def. Solids 157 (2002) 311.
[12] Hj. Matzke, T. Wiss, ITU Annual Report, EUR 19812, 2000.
[13] H. Blank, Hj. Matzke, Rad. Eff. 17 (1973) 57.
[14] J. Soullard, A. Alamo, Rad. Eff. 38 (1978) 133 (in French).
[15] M. Samson, J.P. Grouiller, J. Pavageau, P. Marimbeau, J.M. Vidal, J. Pinel, Proceedings of the 5th International Nuclear Conference on Recycling, Conditioning and Disposal, Nice France, Vol. 3, 1998, p. 986.
[16] C. Poinssot, P. Lovera, C. Ferry, J.M. Gras, Mater. Res. Soc. Symp. Proc. 757 (2002) 35.
[17] R.C. Ewing, W.J. Weber, F.W. Clinard Jr., Progr. Nucl. Energy 29 (2) (1995) 63.
[18] H.S. Carslaw, J.C. Jaeger, Conduction of Heat in Solids, 2nd Ed., Oxford Science Publications, 1959.
[19] Available from: <http://www.insc.anl.gov/matprop/uo2/>.
[20] C. Ferry, P. Lovera, C. Poinssot, L. Johnson, Mater. Res. Soc. Symp. Proc. 807 (2003) 35.